





Cd(II) and Cu(II) coordination polymers based on a multidentate N-donor ligand: syntheses, crystal structures, optical band gaps, and photoluminescence

Wei-Qiu Kan, Shi-Zheng Wen, Hua-You Hu & Yu-He Kan

To cite this article: Wei-Qiu Kan, Shi-Zheng Wen, Hua-You Hu & Yu-He Kan (2015) Cd(II) and Cu(II) coordination polymers based on a multidentate N-donor ligand: syntheses, crystal structures, optical band gaps, and photoluminescence, Journal of Coordination Chemistry, 68:14, 2492-2506, DOI: [10.1080/00958972.2015.1052805](https://doi.org/10.1080/00958972.2015.1052805)



To link to this article: <http://dx.doi.org/10.1080/00958972.2015.1052805>

 View supplementary material 

 Accepted author version posted online: 18 May 2015.
Published online: 14 Jun 2015.

 Submit your article to this journal 

 Article views: 90

 View related articles 

 View Crossmark data 

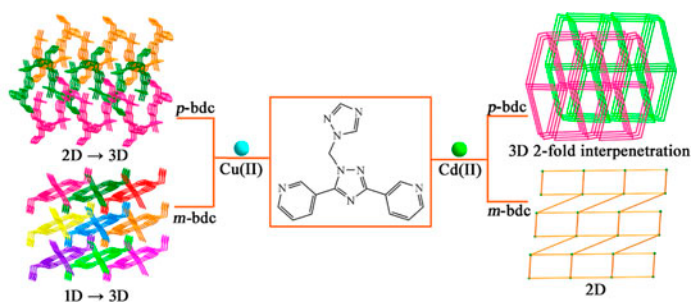
Cd(II) and Cu(II) coordination polymers based on a multidentate N-donor ligand: syntheses, crystal structures, optical band gaps, and photoluminescence

WEI-QIU KAN[†], SHI-ZHENG WEN^{*†‡}, HUA-YOU HU[†] and YU-HE KAN[†]

[†]Jiangsu Province Key Laboratory for Chemistry of Low-Dimensional Materials, School of Chemistry and Chemical Engineering, Huaiyin Normal University, Huaian, PR China

[‡]Huaian Key Laboratory of Functional Materials for Informatics, School of Physics and Electronic Electrical Engineering, Huaiyin Normal University, Huaian, PR China

(Received 30 December 2014; accepted 26 March 2015)



Four Cd(II)- and Cu(II)-containing coordination polymers (CPs) based on a multidentate N-donor ligand and varied dicarboxylate anions, [Cd(3,3'-tmbpt)(*p*-bdc)]·2.5H₂O (**1**), [Cd(3,3'-tmbpt)(*m*-bdc)]·2H₂O (**2**), [Cu(3,3'-tmbpt)(*m*-bdc)]·H₂O (**3**), and [Cu(3,3'-tmbpt)(*p*-bdc)]·2H₂O (**4**), where 3,3'-tmbpt = 1 - ((1*H*-1,2,4-triazol-1-yl)methyl)-3,5-bis(3-pyridyl)-1,2,4-triazole, *p*-H₂bdc = 1,4-benzenedicarboxylic acid, and *m*-H₂bdc = 1,3-benzenedicarboxylic acid, have been prepared hydrothermally. The structures of the compounds were determined by single-crystal X-ray diffraction analyses and further characterized by infrared spectra and elemental analyses. Compound **1** exhibits a 3-D twofold interpenetrating framework with a 6⁵·8 CdSO₄ topology. Compound **2** is a 2-D layer containing meso-helical chains with a 4⁴·6² sql topology. Compound **3** shows a 1-D → 3-D interdigitated architecture while **4** displays a 2-D → 3-D interdigitated architecture. The structural differences of the compounds indicate that the dicarboxylate anions and the central metal ions play important roles in the resulting structures of CPs. Optical band gaps and solid-state photoluminescent properties have also been studied.

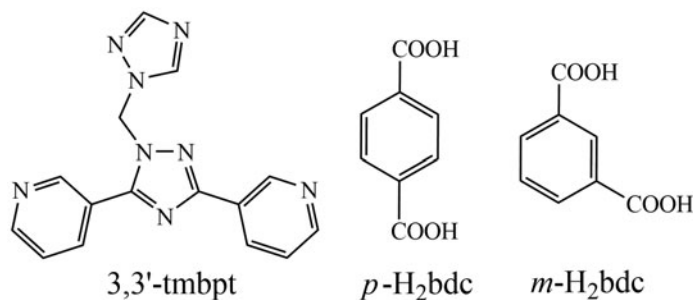
Keywords: Coordination polymer; Multidentate N-donor ligand; Dicarboxylate anion; Optical band gap; Photoluminescence

*Corresponding author. Email: szwen@hytc.edu.cn

1. Introduction

Coordination polymers (CPs) are attracting interest owing to structural diversity and potential applications in air purification, sorption, heterogeneous catalysis, hydrogen storage, and proton conductivity [1–5]. A large number of CPs with interesting structures and valuable applications had been synthesized by employing various multidentate N-donor ligands. For example, the multidentate N-donor ligands hexakis(3-(1,3,4-triazol-1-yl)phenoxy-methyl)benzene [6], hexakis(1,2,4-triazol-ylmethyl)benzene [7], N,N'-bis[5-(2,2-bipyridyl)methyl]-imidazolium bromide [8], and 4'-4-(1,2,4-triazol-1-yl)-phenyl-2,2' : 6',2''-terpyridine [9] have been used to construct CPs with various structures and properties. The final structures of CPs are affected by many factors, such as the coordination geometry preferred by metal ions, the counterions, the pH values, the methods of crystallization, and the structures of ligands [10–13]. The organic anions also play crucial roles in the formation of CPs [14, 15].

Based on the above considerations, we have focused our attention on reactions of metal salts with a multidentate N-donor ligand and investigated the influence of organic anions on the structures of the resultant CPs. In previous work, we synthesized a series of structurally related multidentate N-donor ligands 1-((1*H*-1,2,4-triazol-1-yl)methyl)-3,5-bis(pyridyl)-1,2,4-triazole (tmbpt), which have remarkable features: (i) each tmbpt has two pyridyl and two triazolyl groups, which can afford six potential coordination sites and exhibit various conformations and coordination modes; (ii) each tmbpt has a flexible –CH₂– spacer, which allows the peripheral triazolyl group to bend and rotate freely for conforming to the coordination requirements of metal ions. To extend our work, herein, the multidentate N-donor ligand 1-((1*H*-1,2,4-triazol-1-yl)methyl)-3,5-bis(3-pyridyl)-1,2,4-triazole (3,3'-tmbpt, scheme 1) was employed to react with Cd(II) and Cu(II). By varying the organic dicarboxylate anions, four new CPs, [Cd(3,3'-tmbpt)(*p*-bdc)]·2.5H₂O (**1**), [Cd(3,3'-tmbpt)(*m*-bdc)]·2H₂O (**2**), [Cu(3,3'-tmbpt)(*m*-bdc)]·H₂O (**3**), and [Cu(3,3'-tmbpt)(*p*-bdc)]·2H₂O (**4**) (*p*-H₂bdc = 1,4-benzenedicarboxylic acid and *m*-H₂bdc = 1,3-benzenedicarboxylic acid, scheme 1), were obtained. The structures of the compounds were determined by single-crystal X-ray diffraction analyses and further characterized by infrared spectra (IR) and elemental analyses. Moreover, the effects of dicarboxylate anions and the central metal ions on the structures of the final compounds have been discussed. The optical band gaps and solid-state photoluminescent properties of the compounds have also been studied.



Scheme 1. Organic ligands used in this work.

2. Experimental

2.1. Materials and methods

The 3,3'-tmbpt ligand was synthesized by following a reported approach [16]. Other chemicals and solvents were obtained commercially and used as received. The elemental analyses (C, H, and N) were obtained from a Perkin–Elmer 240 elemental analyzer. IR spectral data were collected on a Mattson Alpha-Centauri spectrometer from 4000 to 400 cm^{-1} . The solid-state photoluminescence spectra of the compounds were recorded by using a Perkin–Elmer FLSP920 spectrometer at room temperature. Diffuse reflectivity spectra were recorded on a Cary 500 spectrophotometer from 200 to 800 nm using BaSO_4 as a standard.

2.2. Syntheses of complexes

2.2.1. Synthesis of $[\text{Cd}(3,3'\text{-tmbpt})(p\text{-bdc})]\cdot 2\text{H}_2\text{O}$ (1). $\text{Cd}(\text{OAc})_2\cdot 2\text{H}_2\text{O}$ (0.081 g, 0.3 mmol), 3,3'-tmbpt (0.03 g, 0.1 mmol), *p*- H_2bdc (0.051 g, 0.3 mmol), NaOH (0.024 g, 0.6 mmol), and 8 mL H_2O were sealed in a 15 mL Teflon reactor and heated at 130 $^\circ\text{C}$ for 3 days. After cooling to ambient temperature at a rate of 10 $^\circ\text{C h}^{-1}$, colorless crystals of **1** were collected in 38% yield. Anal. Calcd for $\text{C}_{23}\text{H}_{21}\text{CdN}_8\text{O}_{6.5}$ ($M_r = 625.88$): C, 44.14; H, 3.38; N, 17.90. Found: C, 44.21; H, 3.49; N, 17.83%. IR (cm^{-1}): 3455 (m), 3129 (w), 1953 (w), 1568 (s), 1390 (s), 1310 (m), 1198 (w), 1130 (m), 1018 (w), 985 (w), 892 (w), 842 (s), 741 (s), 698 (m), 668 (w), 614 (w), 522 (m), 420 (w).

2.2.2. Synthesis of $[\text{Cd}(3,3'\text{-tmbpt})(m\text{-bdc})]\cdot 2\text{H}_2\text{O}$ (2). The preparation of **2** was similar to that of **1**, except that *p*- H_2bdc (0.051 g, 0.3 mmol) was replaced by *m*- H_2bdc (0.051 g, 0.3 mmol). Colorless crystals of **2** were obtained in 33% yield. Anal. Calcd for $\text{C}_{23}\text{H}_{20}\text{CdN}_8\text{O}_6$ ($M_r = 616.87$): C, 44.78; H, 3.27; N, 18.17. Found: C, 44.71; H, 3.19; N, 18.26%. IR (cm^{-1}): 3459 (m), 3116 (w), 1870 (w), 1602 (s), 1555 (s), 1483 (m), 1380 (s), 1272 (w), 1210 (w), 1129 (w), 1072 (w), 1019 (w), 916 (w), 787 (w), 736 (s), 663 (w), 540 (w), 417 (w).

2.2.3. Synthesis of $[\text{Cu}(3,3'\text{-tmbpt})(m\text{-bdc})]\cdot \text{H}_2\text{O}$ (3). The preparation of **3** was similar to that of **2**, except that $\text{Cd}(\text{OAc})_2\cdot 2\text{H}_2\text{O}$ (0.081 g, 0.3 mmol) was replaced by $\text{Cu}(\text{OAc})_2\cdot \text{H}_2\text{O}$ (0.060 g, 0.3 mmol). Blue crystals of **3** were obtained in 22% yield. Anal. Calcd for $\text{C}_{23}\text{H}_{18}\text{CuN}_8\text{O}_5$ ($M_r = 549.99$): C, 50.23; H, 3.30; N, 20.37. Found: C, 50.31; H, 3.21; N, 20.48%. IR (cm^{-1}): 3347 (m), 1865 (w), 1612 (s), 1559 (s), 1477 (w), 1386 (s), 1363 (s), 1269 (w), 1202 (w), 1124 (w), 1037 (w), 879 (w), 817 (w), 759 (m), 717 (m), 577 (w), 419 (w).

2.2.4. Synthesis of $[\text{Cu}(3,3'\text{-tmbpt})(p\text{-bdc})]\cdot 2\text{H}_2\text{O}$ (4). The preparation of **4** was similar to that of **3**, except that *m*- H_2bdc (0.051 g, 0.3 mmol) was replaced by *p*- H_2bdc (0.051 g, 0.3 mmol). Blue crystals of **4** were obtained in 24% yield. Anal. Calcd for $\text{C}_{23}\text{H}_{20}\text{CuN}_8\text{O}_6$ ($M_r = 568.01$): C, 48.63; H, 3.55; N, 19.73. Found: C, 48.50; H, 3.61; N, 19.82%. IR (cm^{-1}): 3478 (m), 3119 (w), 1869 (w), 1571 (s), 1501 (w), 1392 (s), 1312 (w), 1197 (w), 1144 (w), 1101 (w), 1018 (w), 924 (m), 879 (m), 829 (m), 749 (m), 670 (w), 570 (w), 525 (w), 470 (w).

2.3. X-ray crystallography

The crystallographic data were recorded at 293 K from an Oxford Diffraction Gemini R Ultra diffractometer with graphite-monochromated Mo K α radiation ($\lambda = 0.71073$ Å). A multiscan absorption correction was applied. The structures of **1–4** were solved by direct methods of SHELXS-97 [17] and refined by full-matrix least squares techniques employing SHELXL-97 [18]. All the non-H atoms were refined anisotropically. Hydrogens on carbons and water were generated geometrically and refined using a riding model with $d(\text{C–H}) = 0.93\text{--}0.97$ Å, $U_{\text{iso}} = 1.2U_{\text{eq}}(\text{C})$ and $d(\text{O–H}) = 0.85\text{--}0.86$ Å, $U_{\text{iso}} = 1.5U_{\text{eq}}(\text{O})$. Hydrogens of O3W in **1** were not included in the model. The crystallographic data and structure refinement parameters of the compounds are summarized in table 1. Representative bond lengths and angles are in tables S1–S4 (see online supplemental material at <http://dx.doi.org/10.1080/00958972.2015.1052805>).

3. Results and discussion

3.1. Description of the crystal structures

3.1.1. Structure of [Cd(3,3'-tmbpt)(p-bdc)]·25H₂O (1). Compound **1** shows a 3-D twofold interpenetrating framework with a 6⁵·8 CdSO₄ topology (the topologies of **1–4** were analyzed using OLEX [19]). The asymmetric unit of **1** consists of one Cd(II), one 3,3'-tmbpt, two halves of *p*-bdc anion, and two and a half water molecules. As illustrated in figure 1(a), Cd1 is seven-coordinate by two nitrogens from two different 3,3'-tmbpt ligands and five oxygens from two individual *p*-bdc anions and one water molecule in a pentagonal bipyramidal coordination geometry. The Cd–N bond lengths are 2.310(4) and 2.377(4) Å, respectively. The Cd–O bond lengths are 2.344(4)–2.450(5) Å (table S1). Each 3,3'-tmbpt coordinates to two Cd(II) ions to form an infinite chain [figure 1(b)]. The *p*-bdc anions are bidentate, connecting the chains to generate a 3-D framework [figure 1(c)]. All carboxylate

Table 1. Crystal data and structure refinements for **1–4**.

	1	2	3	4
Formula	C ₂₃ H ₂₁ CdN ₈ O _{6.5}	C ₂₃ H ₂₀ CdN ₈ O ₆	C ₂₃ H ₁₈ CuN ₈ O ₅	C ₂₃ H ₂₀ CuN ₈ O ₆
Formula weight	625.88	616.87	549.99	568.01
Crystal system	Orthorhombic	Monoclinic	Monoclinic	Monoclinic
Space group	<i>Pcnb</i>	<i>P2₁/n</i>	<i>C2/c</i>	<i>P2₁/n</i>
<i>a</i> (Å)	10.899(3)	10.070(4)	17.580(8)	10.819(5)
<i>b</i> (Å)	18.363(7)	23.375(10)	15.730(8)	14.454(7)
<i>c</i> (Å)	25.401(4)	10.302(4)	17.456(7)	15.564(10)
α (°)	90	90	90	90
β (°)	90	96.679(3)	92.433(4)	101.204(5)
γ (°)	90	90	90	90
<i>V</i> (Å ³)	5084(3)	2408.5(17)	4823(4)	2387(2)
<i>Z</i>	8	4	8	4
<i>D</i> _{calc} (g cm ⁻³)	1.635	1.701	1.515	1.580
<i>F</i> (0 0 0)	2520	1240	2248	1164
Reflections (collected/unique)	20,568/5972	18,367/5839	10,941/5497	10,336/5515
<i>R</i> _{int}	0.0358	0.0469	0.0610	0.0648
Goodness-of-fit (GOF) on <i>F</i> ²	1.210	1.051	1.010	0.970
<i>R</i> ₁ [<i>I</i> > 2 σ (<i>I</i>)]	0.0600	0.0448	0.0706	0.0647
<i>wR</i> ₂ [all data]	0.1441	0.0941	0.1747	0.1201

groups of the *p*-bdc anions adopt the $\mu_1 - \eta^1 : \eta^1$ coordination mode (mode 1 in scheme S1, the subscript of μ represents the number of metal ions coordinating to each carboxylate group of the bdc anion and the superscript η represents the number of metal ions coordinating to each oxygen of one carboxylate group).

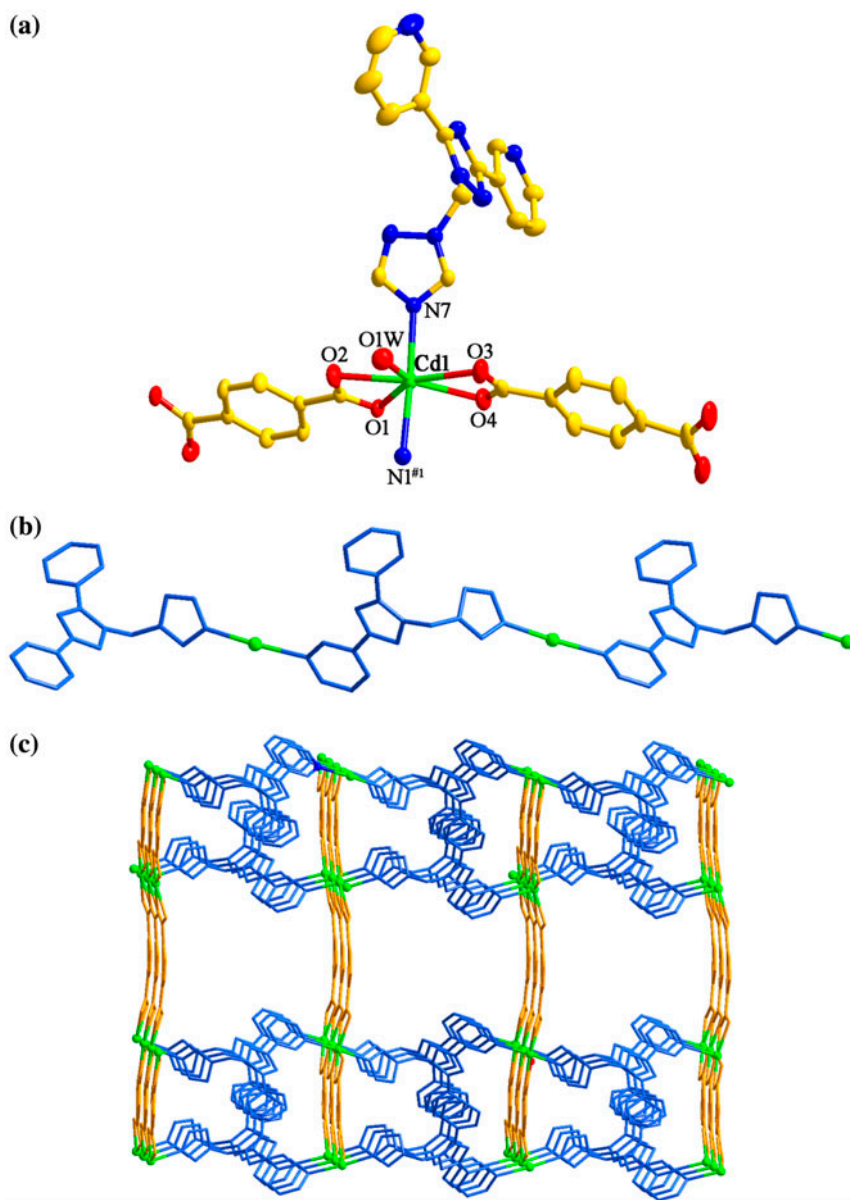


Figure 1. (a) Coordination environment of Cd(II) with hydrogens and lattice water molecules omitted for clarity (30% probability displacement ellipsoids). Symmetry code: #1 $-x + 1/2, y, z - 1/2$. (b) View of the chain formed by Cd(II) ions and 3,3'-tmbpt ligands in **1**. (c) View of the 3-D framework of **1**. (d) View of the twofold interpenetrating framework of **1**.

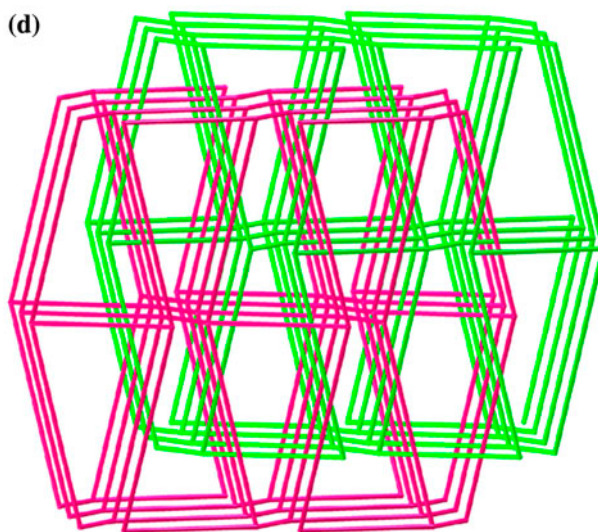


Figure 1. (Continued).

From a topological point of view, each Cd(II) can be considered as a four-connected node, and the 3,3'-tmbpt ligands and the *p*-bdc anions can be reduced to linkers. Thus, the whole 3-D framework can be simplified as a four-connected framework with a $6^5 \cdot 8$ CdSO₄ topology. Two identical frameworks interpenetrate each other, giving a twofold interpenetrating framework [figure 1(d)].

3.1.2. Structure of [Cd(3,3'-tmbpt)(*m*-bdc)]·2H₂O (2). Single-crystal X-ray diffraction analysis reveals that **2** displays a 2-D layered structure. The asymmetric unit of **2** contains one Cd(II), one 3,3'-tmbpt, one *m*-bdc anion, and two water molecules. As shown in figure 2(a), Cd1 is six-coordinate in a distorted octahedral coordination geometry, defined by two nitrogens from two 3,3'-tmbpt ligands and four oxygens from two individual *m*-bdc anions and one water. The Cd–N bond distances are 2.345(3) and 2.389(3) Å, respectively. The Cd–O bond distances vary from 2.268(2) to 2.476(3) Å (table S2). Each 3,3'-tmbpt coordinates to two Cd(II) ions to form a single-stranded meso-helical chain [figure 2(b)]. Meso-helical chain, which has alternating right and left helical parts, is not a helical structure because the strand contains an inversion center and does not have defined chirality [20]. The meso-helical chains are further connected by the *m*-bdc anions to form a 2-D layered structure [figure 2(c)]. The carboxylate groups of *m*-bdc anion adopt $\mu_1 - \eta^1 : \eta^1$ and $\mu_1 - \eta^1 : \eta^0$ coordination modes (mode 2 in scheme S1), respectively.

Topologically, the Cd(II) ions can be viewed as 4-connected nodes, and the 3,3'-tmbpt ligands and the *m*-bdc anions can be regarded as linkers. The whole layer can be simplified as a 4-connected net with a $4^4 \cdot 6^2$ sql topology [figure 2(d)].

3.1.3. Structure of [Cu(3,3'-tmbpt)(*m*-bdc)]·H₂O (3). Compound **3** shows a 1-D → 3-D interdigitated architecture. The asymmetric unit of **3** consists of one Cu(II), one 3,3'-tmbpt,

one *m*-bdc anion, and one water. Figure 3(a) shows the coordination environment of Cu(II). Cu1 is five-coordinate in a trigonal bipyramidal coordination geometry, furnished by two nitrogens from two distinct 3,3'-tmbpt ligands and three oxygens from two different *m*-bdc anions and one water molecule. The Cu–N bond lengths are 2.036(4) and 2.062(4) Å, respectively. The Cu–O bond lengths vary from 1.925(3) to 2.392(4) Å. The Cu–N and Cu–O bond lengths are in normal ranges as other Cu(II)-containing CPs [21–23]. The 3,3'-tmbpt ligands and the *m*-bdc anions both are bidentate, linking the Cu(II) ions to form two kinds of wave-like chains by sharing the same Cu(II) ions [figure 3(b)]. The carboxylate groups of the *m*-bdc anion adopt the $\mu_1 - \eta^1 : \eta^0$ coordination mode (mode 3 in scheme S1). Interestingly, an example of 1-D \rightarrow 3-D interdigitation is observed in **3**, where each chain is digitated directly by one adjacent chain through the uncoordinated triazolyl group [figure 3(c)].

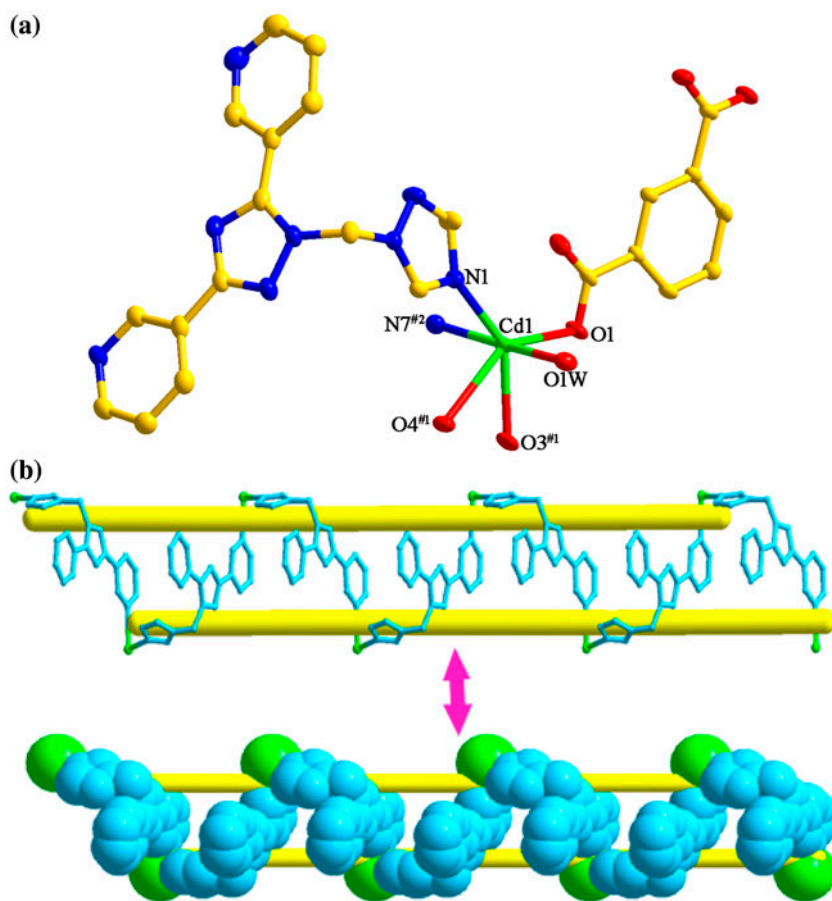


Figure 2. (a) Coordination environment of Cd(II) with hydrogens and lattice waters omitted for clarity (30% probability displacement ellipsoids). Symmetry codes: #1 $x, y, z - 1$; #2 $x - 1/2, -y + 1/2, z + 1/2$. (b) View of the meso-helical chain formed by Cd(II) ions and the 3,3'-tmbpt ligands in **2**. (c) View of the layer of **2**. (d) View of the four-connected net with a $4^4.6^2$ sq1 topology.

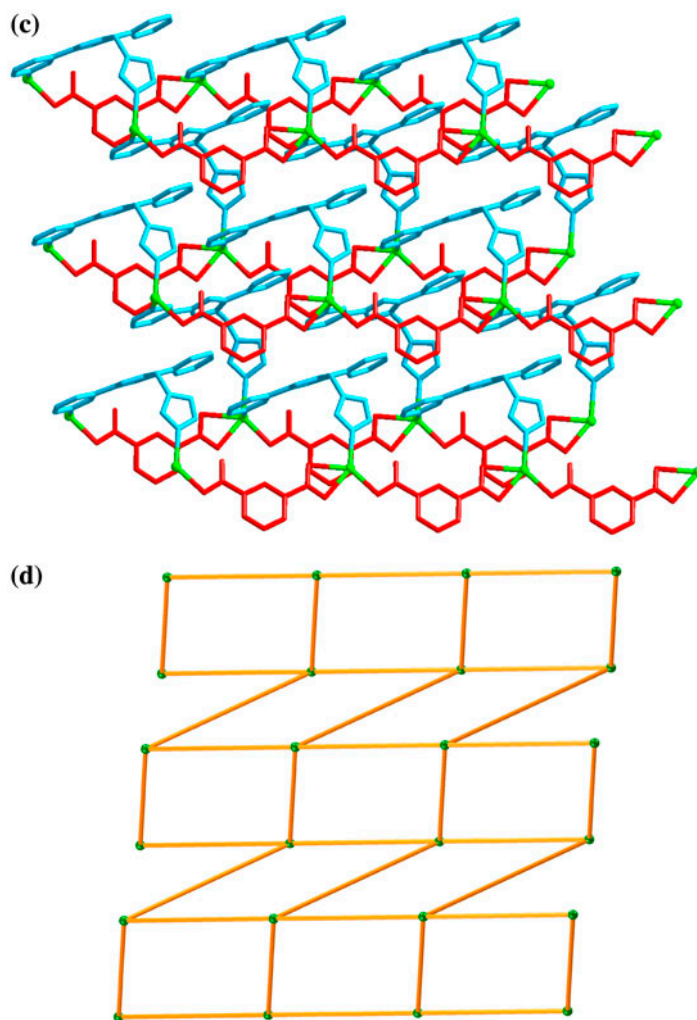


Figure 2. (Continued).

3.1.4. Structure of $[\text{Cu}(3,3'\text{-tmbpt})(p\text{-bdc})]\cdot 2\text{H}_2\text{O}$ (4). Compound 4 displays a 2-D \rightarrow 3-D interdigitated architecture. The asymmetric unit of 4 consists of one Cu(II), one 3,3'-tmbpt, one *p*-bdc anion, and two water molecules. As shown in figure 4(a), Cu1 is five-coordinate with two nitrogens from two different 3,3'-tmbpt ligands and three oxygens from two different *p*-bdc anions and one water in a trigonal bipyramidal coordination geometry. The Cu–N bond distances are 2.045(3) and 2.332(4) Å, respectively. The Cu–O bond lengths range from 1.943(3) to 2.007(3) Å. Each 3,3'-tmbpt is a bidentate linker, connecting the Cu(II) ions to generate a wave-like chain [figure 4(b)]. The chains are further connected by *p*-bdc anions to form a layer [figure 4(c)]. The two carboxylate groups of the *p*-bdc anion adopt $\mu_1 - \eta^1 : \eta^0$ coordination (mode 4 in scheme S1).

Topologically, if the Cu(II) ions can be regarded as four-connected nodes, and the 3,3'-tmbpt ligands and the *p*-bdc anions can be viewed as linkers, the layer can be simplified as

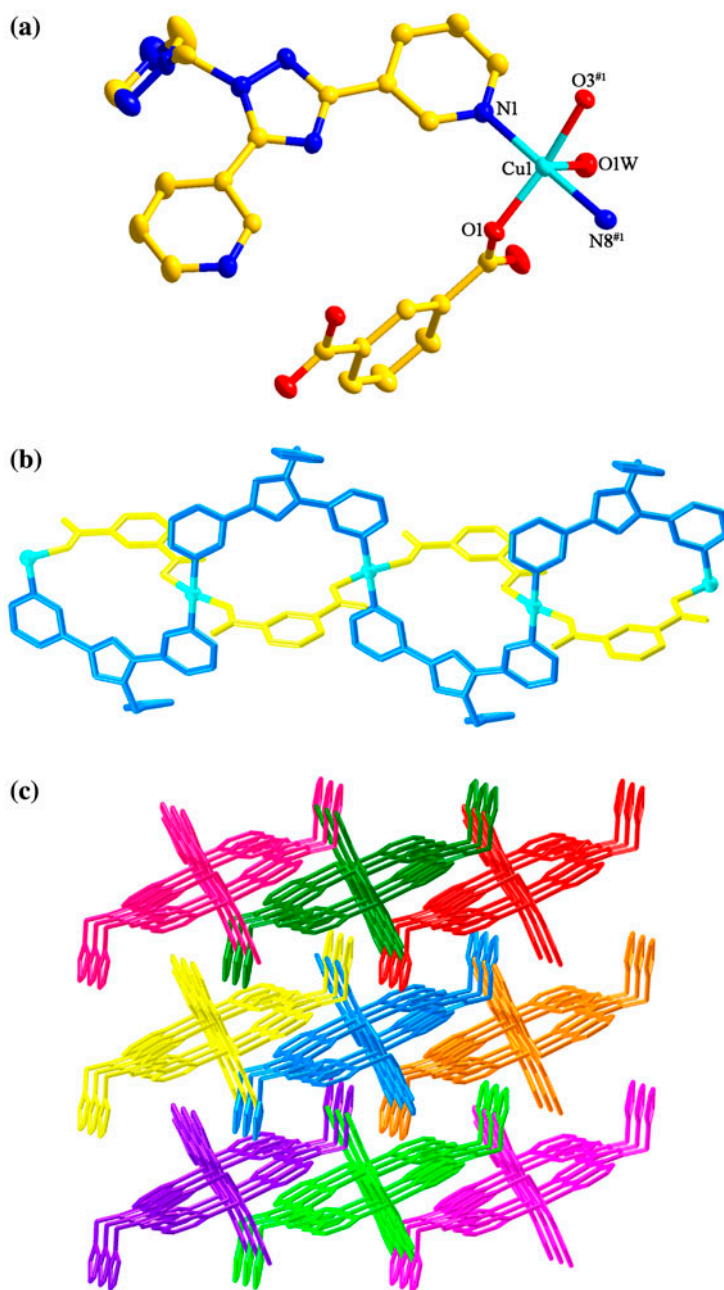


Figure 3. (a) Coordination environment of Cu(II) with hydrogens omitted for clarity (30% probability displacement ellipsoids). Symmetry code: #1 $-x + 1/2, y - 1/2, -z + 1/2$. (b) View of the chain of **3**. (c) View of the 1D \rightarrow 3D interdigitated architecture of **3**.

a four-connected net with a $4^4 \cdot 6^2$ sql topology [figure 4(d)]. Moreover, an example of 2-D \rightarrow 3-D interdigitation is observed in **4**, where each layer is digitated directly by one adjacent layer through the uncoordinated triazolyl group [figure 4(e)]. Interdigitated structures are extended arrays in which individual motifs interweave like the fingers of folded hands. Interdigitated structures usually include 0-D \rightarrow 2-D, 1-D \rightarrow 2-D, 1-D \rightarrow 3-D, 2-D \rightarrow 2-D, and 2-D \rightarrow 3-D architectures [24–28]. This research gave two more structures to the examples of interdigitated arrays.

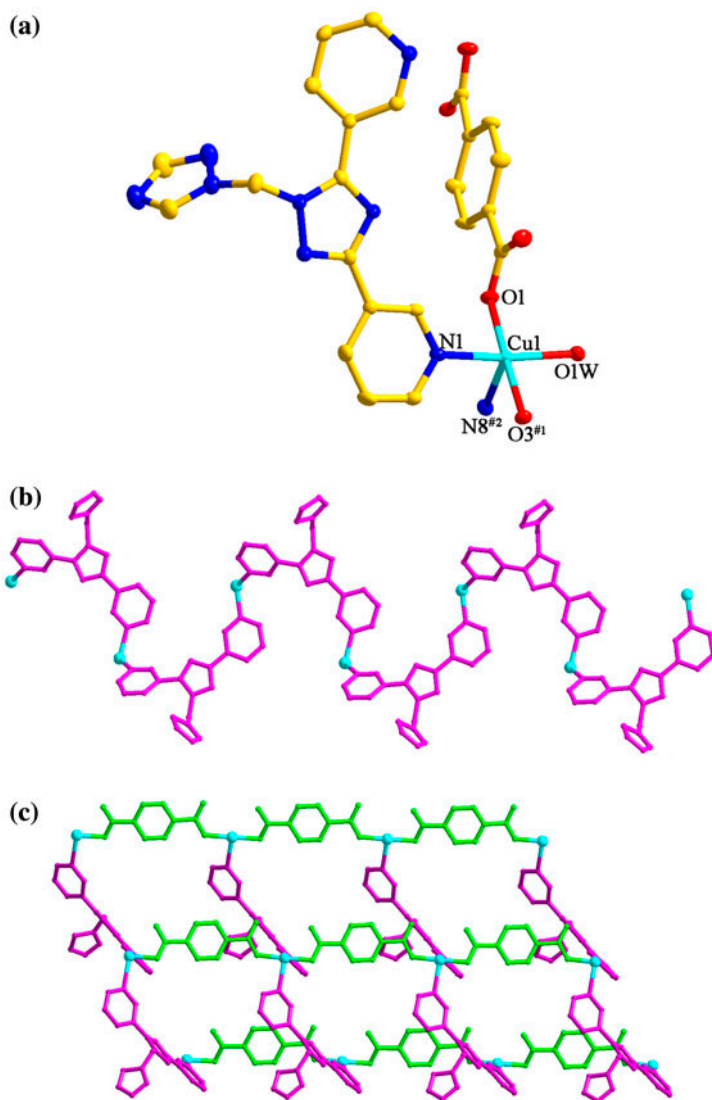


Figure 4. (a) Coordination of Cu(II) with hydrogens and lattice waters omitted for clarity (30% probability displacement ellipsoids). Symmetry codes: #1 $x + 1, y, z$; #2 $x + 1/2, -y + 1/2, z + 1/2$. (b) View of the wave-like chain formed by Cu(II) and 3,3'-tmbpt ligands. (c) View of layer of **4**. (d) View of the four-connected net with a $4^4 \cdot 6^2$ sql topology. (e) View of the 2-D \rightarrow 3-D interdigitated architecture of **4**.

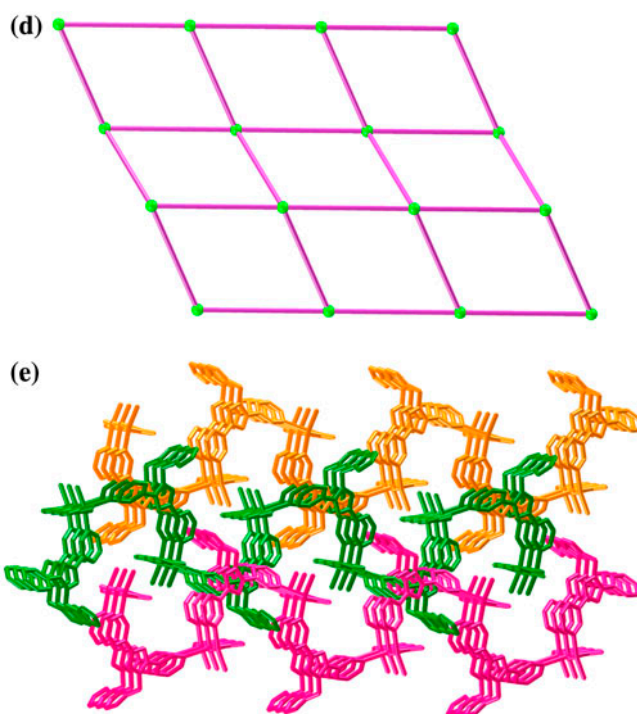


Figure 4. (Continued).

3.2. Effects of dicarboxylate anions on structures of the compounds

The dicarboxylate anions play important roles in the determination of the structures of CPs. The structural differences of $[\text{Cd}(3,3'\text{-tmbpt})(p\text{-bdc})]\cdot 2.5\text{H}_2\text{O}$ (**1**) and $[\text{Cd}(3,3'\text{-tmbpt})(m\text{-bdc})]\cdot 2\text{H}_2\text{O}$ (**2**), as well as $[\text{Cu}(3,3'\text{-tmbpt})(m\text{-bdc})]\cdot \text{H}_2\text{O}$ (**3**) and $[\text{Cu}(3,3'\text{-tmbpt})(p\text{-bdc})]\cdot 2\text{H}_2\text{O}$ (**4**), are clearly related to the structures of the dicarboxylate anions. In **1** and **2**, cadmium and the N-donor ligands are the same, and the only difference is the carboxylate. Although the aromatic dicarboxylate anions *m*-bdc and *p*-bdc both are μ_2 -bridges, the two carboxylate groups of *m*-bdc are located in the 1,3-positions of benzene ring with an angle of about 120° , whereas those of *p*-bdc are in the 1,4-positions with an angle of 180° . The different angles between the two carboxylate groups in *m*-bdc and *p*-bdc anions lead to their coordination with the Cd(II) ions in different directions and coordination modes. In **1**, each *p*-bdc anion connects two Cd(II) ions to form a wave-like chain with the Cd \cdots Cd distance of about 11.2 Å. All the carboxylate groups of the *p*-bdc anions adopt the $\mu_1 - \eta^1 : \eta^1$ coordination mode. Further, the chains are linked by the 3,3'-tmbpt ligands to generate a 3-D twofold interpenetrating framework. In **2**, each *m*-bdc anion connects two Cd(II) ions to form a wave-like chain with the shorter Cd \cdots Cd distance of about 10.3 Å. The carboxylate groups of *m*-bdc anion adopt $\mu_1 - \eta^1 : \eta^1$ and $\mu_1 - \eta^1 : \eta^0$ coordination modes, respectively. The chains are connected by 3,3'-tmbpt ligands to form a 2-D four-connected net with a $4^4\cdot 6^2$ sql topology. It is clear that the dicarboxylate anions affect the final structures of the compounds.

3.3. Effects of central metals on structures of the compounds

Central metals also have a remarkable function in the formation of the final structures. Compounds $[\text{Cd}(3,3'\text{-tmbpt})(p\text{-bdc})]\cdot 2.5\text{H}_2\text{O}$ (**1**) and $[\text{Cu}(3,3'\text{-tmbpt})(p\text{-bdc})]\cdot 2\text{H}_2\text{O}$ (**4**), as well as $[\text{Cd}(3,3'\text{-tmbpt})(m\text{-bdc})]\cdot 2\text{H}_2\text{O}$ (**2**) and $[\text{Cu}(3,3'\text{-tmbpt})(m\text{-bdc})]\cdot \text{H}_2\text{O}$ (**3**), show the effects of the central metals on the structures of CPs. The differences in the coordination numbers of the central metals are the main reasons for the structural differences. Because the radius of the Cu(II) ion is smaller than Cd(II), the coordination number of Cu(II) is lower. The coordination numbers of the Cd(II) ions in **1** and **2** are 7 and 6, respectively. However, the Cu(II) ions in **3** and **4** show coordination numbers of 5. The different coordination numbers of the Cd(II) ion and Cu(II) ion lead to their coordination with the organic ligands in different coordination geometries. Compounds **2** and **3** provide examples. In **2**, each Cd(II) is octahedral with the two 3,3'-tmbpt ligands and the two *p*-bdc anions locating in the axial positions. Thus, the Cd(II) ions are linked by the 3,3'-tmbpt ligands and the *p*-bdc anions to generate a 2-D layer structure. However, in **3**, each Cu(II) is a trigonal bipyramid with the two 3,3'-tmbpt ligands and the two *p*-bdc anions in *trans* positions. Thus, the Cu(II) ions are linked by 3,3'-tmbpt ligands and the *p*-bdc anions to generate a 1-D chain. Further, a 3-D supramolecular architecture is formed by the 1-D interdigitated chains. It is obvious that the central metals affect the final structures of the compounds.

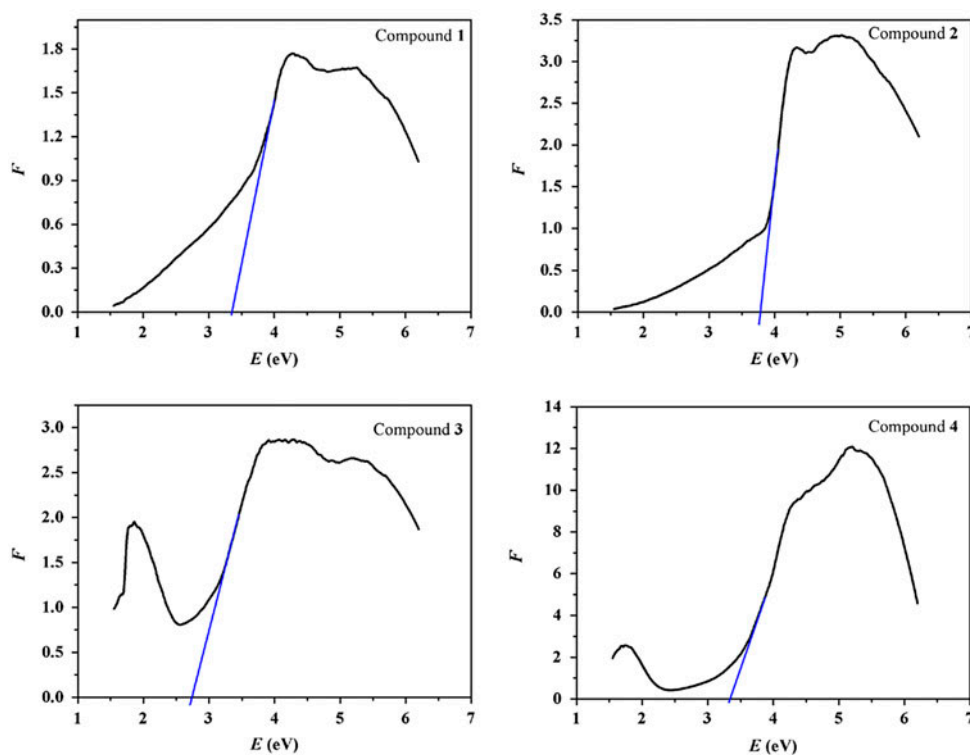


Figure 5. F vs. E plots of **1–4** converted from diffuse reflectivity spectra.

3.4. IR spectra

Compounds **1–4** show O–H stretches of water at 3455, 3459, 3347, and 3478 cm^{-1} , respectively. The asymmetric and symmetric stretching vibrations of the carboxylates of **1–4** are observed in the ranges of 1555–1612 and 1363–1483 cm^{-1} , respectively. The absence of strong absorptions around 1700 cm^{-1} implies complete deprotonation of the carboxylic groups in **1–4**.

3.5. Optical band gaps

Recently, a number of CPs have been reported to be promising semiconductive materials [29–31]. We, thus, studied the conductivities of **1–4**. Diffuse reflectance spectral data were collected to achieve the band gaps (E_g) of **1–4**. The E_g was confirmed as the intersection point between the energy axis and the line extrapolated from the linear portion of the adsorption edge in a plot of the Kubelka–Munk function ($F = (1 - R)^2/2R$, R is the reflectivity at a certain wavelength) F against E as reported in the literature [29–31]. The F against E plots are shown in figure 5, from which it can be found that the E_g values of **1–4** are 3.36, 3.78, 2.74, and 3.35 eV, respectively. The E_g values imply the nature of semiconductivities for **1–4**.

3.6. Photoluminescence

CPs with Cd(II) metal centers have diverse applications in display, lighting, sensing, and optical devices [32]. Therefore, in this work, the photoluminescent properties of the free organic ligands, **1** and **2** have been studied in the solid state at room temperature (figure 6).

The free 3,3'-tmbpt, *m*-H₂bdc, and *p*-H₂bdc show emission peaks at 421/537, 390, and 393 nm, respectively [33]. These emission peaks may be caused by the π^*-n or $\pi^*-\pi$ transition as previously reported [34, 35]. Upon complexation of the organic ligands with the Cd(II) ions, the emission peaks are observed at 397 nm for **1** and 442 nm for **2**. Because Cd(II) has a d^{10} configuration, it is difficult to oxidize or reduce. Therefore, the emissions of **1** and **2** are neither metal-to-ligand charge transfer nor ligand-to-metal charge transfer [36]. For **1**, the emission should originate from *m*-bdc anion, because similar emission is

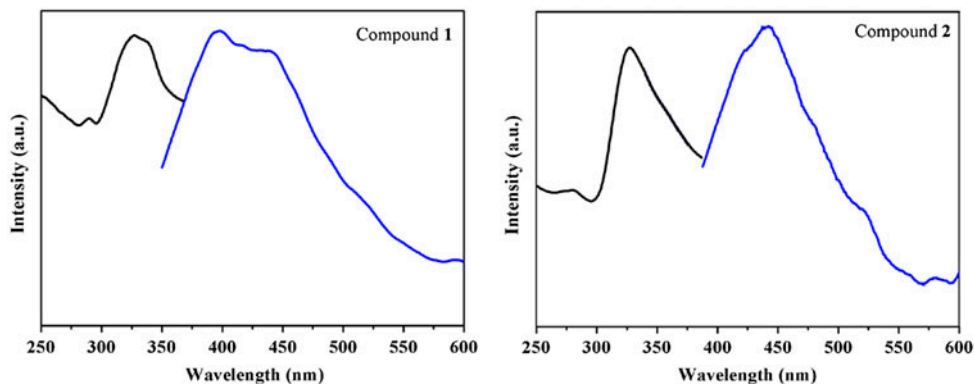


Figure 6. Solid-state fluorescence spectra of **1** and **2**.

observed for *m*-H₂bdc [37]. For **2**, the emission peak can be attributed to the $\pi^*-\pi$ transition of the 3,3'-tmbpt ligand, because a similar peak appears for free 3,3'-tmbpt ligand [38].

4. Conclusion

Four CPs based on 3,3'-tmbpt and structurally related dicarboxylate anions have been synthesized hydrothermally. These compounds display different structures, which indicate that the central metals and the organic anions play important roles in determination of the final structures of CPs. The optical band gaps of the compounds reveal that these compounds are potential semi-conductive materials. Solid-state luminescence spectra indicate that **1** and **2** have photoluminescent properties at room temperature.

Supplementary material

X-ray crystallographic files (CIF) and selected bond lengths and angles of the compounds. Crystallographic data for the structures reported in this article have been deposited with the Cambridge Crystallographic Data Center, CCDC Nos. 1041165–1041168. Supplementary data associated with this article can be found in the online version.

Disclosure statement

No potential conflict of interest was reported by the authors.

Funding

This work was supported by the National Natural Science Foundation of China [grant number 21401063], [grant number 21403081]; the Jiangsu Province NSF [grant number BK20140452], [grant number BK20140453]; and the Open Fund of Jiangsu Key Laboratory for Chemistry of Low-dimensional Materials [grant number JSKC13137].

References

- [1] J.B. DeCoste, G.W. Peterson. *Chem. Rev.*, **114**, 5695 (2014).
- [2] N.C. Burtch, H. Jasuja, K.S. Walton. *Chem. Rev.*, **114**, 10575 (2014).
- [3] M. Zhao, S. Ou, C.D. Wu. *Acc. Chem. Res.*, **47**, 1199 (2014).
- [4] Y. Yan, S.H. Yang, A.J. Blake, M. Schröder. *Acc. Chem. Res.*, **47**, 296 (2014).
- [5] M. Sadakiyo, T. Yamada, H. Kitagawa. *J. Am. Chem. Soc.*, **136**, 13166 (2014).
- [6] W. Wang, W.Q. Kan, J. Yang, J.F. Ma. *CrystEngComm*, **15**, 3824 (2013).
- [7] Z. Zhang, J.F. Ma, Y.Y. Liu, W.Q. Kan, J. Yang. *CrystEngComm*, **15**, 2009 (2013).
- [8] F.J. Cui, P.J. Yang, X.J. Huang, X.J. Yang, B. Wu. *Organometallics*, **31**, 3512 (2012).
- [9] P. Wang, L. Luo, T. Okamura, H.P. Zhou, W.Y. Sun, Y.P. Tian. *Polyhedron*, **44**, 18 (2012).
- [10] J.K. Sun, W. Li, L.X. Cai, J. Zhang. *CrystEngComm*, **13**, 1550 (2011).
- [11] P.X. Yin, J. Zhang, Y.Y. Qin, J.K. Cheng, Z.J. Li, Y.G. Yao. *CrystEngComm*, **13**, 3536 (2011).
- [12] M. Chen, S.S. Chen, T. Okamura, Z. Su, M.S. Chen, Y. Zhao, W.Y. Sun, N. Ueyama. *Cryst. Growth Des.*, **11**, 1901 (2011).
- [13] B. Li, G. Li, D. Liu, Y. Peng, X. Zhou, J. Hua, Z. Shi, S. Feng. *CrystEngComm*, **13**, 1291 (2011).
- [14] H.Y. Lin, J. Luan, X.L. Wang, G.C. Liu, A.X. Tian, J.W. Zhang. *J. Coord. Chem.*, **68**, 71 (2015).
- [15] P.W. Liu, C.P. Li, Y. Bi, J. Chen. *J. Coord. Chem.*, **66**, 2012 (2013).
- [16] W.Q. Kan, B. Liu, J. Yang, Y.Y. Liu, J.F. Ma. *Cryst. Growth Des.*, **12**, 2288 (2012).
- [17] G.M. Sheldrick. *SHELXS-97, Programs for X-ray Crystal Structure Solution*, University of Göttingen, Göttingen (1997).

- [18] G.M. Sheldrick. *SHELXL-97, Programs for X-ray Crystal Structure Refinement*, University of Göttingen, Göttingen (1997).
- [19] O.V. Dolomanov, A.J. Blake, N.R. Champness, M.J. Schröder. *Appl. Crystallogr.*, **36**, 1283 (2003).
- [20] S. Wang, H.Y. Zang, C.Y. Sun, G.J. Xu, X.L. Wang, K.Z. Shao, Y.Q. Lan, Z.M. Su. *CrystEngComm*, **12**, 3458 (2010).
- [21] Z. Zhang, D.F. Wu, K. Hu, Y.J. Shi, Z.L. Chen, F.P. Liang. *J. Coord. Chem.*, **66**, 2499 (2013).
- [22] L. Tian, S.Y. Zhou. *J. Coord. Chem.*, **66**, 2863 (2013).
- [23] L. Zhao, F. Guo. *J. Coord. Chem.*, **66**, 2940 (2013).
- [24] D.W. Zhang, G.Y. Zhao. *Synth. React. Inorg. Met.-Org. Chem.*, **45**, 524 (2015).
- [25] S.B. Li, H.Y. Ma, H.J. Pang, L. Zhang. *Cryst. Growth Des.*, **14**, 4450 (2014).
- [26] Y.Y. Yang, Z.J. Lin, T.T. Liu, J. Liang, R. Cao. *CrystEngComm*, **17**, 1381 (2015).
- [27] Y.X. Zhang, J. Yang, W.Q. Kan, J.F. Ma. *CrystEngComm*, **14**, 6004 (2012).
- [28] Y.H. Luo, B. Li, X.Y. Yu, C.M. Han, X.X. Lu, H. Zhang, X. Chen. *Polyhedron*, **85**, 705 (2014).
- [29] J. Guo, J.F. Ma, B. Liu, W.Q. Kan, J. Yang. *Cryst. Growth Des.*, **11**, 3609 (2011).
- [30] H.S. Liu, Y.Q. Lan, S.L. Li. *Cryst. Growth Des.*, **10**, 5221 (2010).
- [31] B. Liu, Z.T. Yu, J. Yang, W. Hua, Y.Y. Liu, J.F. Ma. *Inorg. Chem.*, **50**, 8967 (2011).
- [32] Y. Cui, Y. Yue, G. Qian, B. Chen. *Chem. Rev.*, **112**, 1126 (2012).
- [33] W.Q. Kan, J. Yang, Y.Y. Liu, J.F. Ma. *CrystEngComm*, **14**, 6934 (2012).
- [34] K.H. He, Y.W. Li, Y.Q. Chen, W.C. Song, X.H. Bu. *Cryst. Growth Des.*, **12**, 2730 (2012).
- [35] L.J. Li, C. Qin, X.L. Wang, K.Z. Shao, Z.M. Su, P.J. Liu. *CrystEngComm*, **14**, 4205 (2012).
- [36] L.P. Zhang, J.F. Ma, J. Yang, Y.Y. Pang, J.C. Ma. *Inorg. Chem.*, **49**, 1535 (2010).
- [37] X.Y. Hou, X. Wang, F. Fu, J.J. Wang, L. Tang. *J. Coord. Chem.*, **66**, 3126 (2013).
- [38] Y.Y. Liu, Z.H. Wang, J. Yang, B. Liu, Y.Y. Liu, J.F. Ma. *CrystEngComm*, **13**, 3811 (2011).